Molecular-dynamics study of incommensurate phases in a three-dimensional crystal

K. Parlinski*

Institut für Festkörperforschung, Kernforschungsanlage, D-5170 Jülich, Germany
and Laboratoire de Physique des Solides, Université Paris–Sud, 91405 Orsay, France

F. Dénoyer

Laboratoire de Physique des Solides, Université Paris–Sud, 91405 Orsay, France

G. Eckold

Institut für Festkörperforschung, Kernforschungsanlage, D-5170 Jülich, Germany
and Institut für Kristallographie der Rheinisch-Westfälische Technische Hochschule, Aachen, Germany

Two cases of the three-dimensional model—one with incommensurate phases and another with commensurate phases only—have been simulated with use of the molecular-dynamics method. The model crystallite has been subjected to periodic boundary conditions. In the incommensurate regime the phase-transition mechanism consists of nucleation and growth of stripples and antistripples, having the structure described by the domains of the closest reference commensurate phase. The stripple mechanism could not describe the phase transition in the commensurate regime.

I. INTRODUCTION

Close to the lock-in phase transition, the incommensurate phase can be considered as an ordered sequence of domains of a reference commensurate phase, separated by discommensuration planes. This reference phase must be stable in some temperature interval and is characterized by a commensurate wave vector which differs from the incommensurate one by a small fraction of a reciprocal-lattice vector.

In incommensurate crystals the characteristic wave vector of the modulation changes as a function of temperature or other external parameters. These changes are consequences of crystal-lattice reconstruction. It is believed that in crystals with one-dimensional modulation the reconstruction occurs via the stripple mechanism.[1-3] A stripple is a topological defect built up from domains of the reference commensurate phase. The domains of the stripple are separated by discommensuration planes. These planes are bounded by a closed curve called a deperiodization line.[3] In a superheated or undercooled crystal a stripple is nucleated by thermal fluctuations; later it grows by lateral motion of the deperiodization line adding to the system one period of the modulation and a definite number of discommensuration planes. The antistripples are nucleated in the reverse process, when the discommensuration planes are removed from the system. The antistripple is bordered by a deperiodization line as well and each removes from the system one period of the modulation. Stripples or antistripples appear when the wave vector shifts away from or toward the reference commensurate phase, respectively.

The purpose of the present work is to simulate, in *three-dimensional* system, the microscopic mechanism of the kinetic reconstruction of the incommensurate modulation. With simulations one could demonstrate the existence of stripples, visualize their propagation, analyze the structure of stripples, and relate the temperature anomalies observed in the kinetic run to the nucleation of stripples. The results also led to the conclusion that the phase transition between two commensurate phases cannot be described by the stripple mechanism.

There is a number of experimental facts which are consequences of the stripple mechanism: Namely, the global thermal hysteresis observed in the temperature dependence of the modulation wave vector,[4] dielectric constant[5] and birefringence[6] measurements, the hysteresis at the commensurate-incommensurate phase transition[7,8] and the shape of the satellite pattern which has been quite recently determined in the real-time kinetic experiment, on rather short time scales, by time-resolved neutron diffraction technique.[9] Moreover, stripples have been already directly observed with an electron-microscopic technique in crystals of $2H$-TaSe$_2$,[10,11] Rb$_2$ZnCl$_4$,[12] sodium barium niobate,[13] and TMATC-Zn.[14] A computer simulation of a two-dimensional system also confirms the existence of stripples.[3,15,16] Objects topologically equivalent to stripples have been seen in the two-dimensional pattern of convective rolls in an anisotropic fluid: a nematic liquid crystal subjected to an ac electric field.[17]

In Sec. II two cases of a simple three-dimensional model are defined: an incommensurate and a commensurate one. Then, we specify the conditions needed to produce a minimum in the potential energy along a high-symmetry direction of the reciprocal lattice, which is necessary to make the one-dimensional modulation stable. In order to study the kinetics of the model we formulate the procedure which allows us to change the wave vector of the dispersion-curve minimum and consequently the characteristic wave vector of the modulation. Because of the rather small size of the system, we have applied periodic

boundary conditions which discretize the allowed wave vectors of the modulation and prevent nucleation of the stripples at the surfaces of the crystal.[18] Only a few essential facts about the molecular-dynamics method are given. In Sec. III we report the results of the simulation. Our study of the incommensurate model generally confirm the stripple mechanism. They also show the multidomain structure of the stripples for wave vectors close to commensurate ones. As the wave vector moves further away from a commensurate value, specially in the middle region of the wave vector in between two reference commensurate phases, one still observes stripples, but their description by domains is no longer useful. We find that the nucleation and growth of stripples (antistripples), driving the metastable state toward an equilibrium, always decrease the potential energy (i.e., release heat) and thus increase the temperature of the system.

Simulations of the commensurate model showed that stripples do not appear in the phase transition between two commensurate phases and that the transition mechanism is more closely associated with a modification of particle displacements within layers of the crystal perpendicular to the modulation direction, than with the production of stripples.

II. MODEL

The model we consider is a three-dimensional simple tetragonal lattice with one particle per unit cell. Each particle has one degree of freedom, which is a displacement in the z direction denoted by $u(i,j,l)$. A particle is harmonically coupled to its nearest neighbors and, along the z axis, also to its next-nearest neighbors. Furthermore, each particle moves in an anharmonic local potential. The potential energy of the model is taken to be

$$V = \frac{1}{2}\sum_{i,j,l}\{Au^2(i,j,l) + Gu^4(i,j,l) + Bu(i,j,l)[u(i,j,l+1) + u(i,j,l-1)] + Du(i,j,l)[u(i,j,l+2) + u(i,j,l-2)]$$

$$+ Cu(i,j,l)[u(i+1,j,l) + u(i-1,j,l)] + u(i,j+1,l) + u(i,j-1,l)\} .$$

(2.1)

A one-dimensional chain of this kind (with $C=0$) has been already studied[19,20] as a function of parameters A, B, and D. We may study three-dimensional version by the molecular-dynamics technique. Another choice could be to simulate the well-known ANNNI model,[21] but since it is an Ising-spinlike model, its dynamics is not uniquely determined.

The harmonic part of the potential energy (2.1) can be transformed into a diagonal form[3] and its corresponding dispersion curve is given by

$$\omega^2(\mathbf{k}) = A + 2B\cos(2\pi k_z c) + 2D\cos(4\pi k_z c)$$

$$+ 2C[\cos(2\pi k_x a) + \cos(2\pi k_y a)] .$$

(2.2)

Here $\mathbf{k} = (k_x, k_y, k_z)$ is the wave vector in three-dimensional reciprocal space and a and c are lattice constants. The model possesses one single branch with nonzero frequency at the Brillouin-zone center. In order to form a one-dimensional incommensurate modulation in the z direction, the minimum of the dispersion curve $\omega^2(\mathbf{k})$ should occur along the [001] direction. Let us denote the wave vector of this minimum by $(0,0,k_p)$. The incommensurate or commensurate modulation is characterized by the wave vector $(0,0,k_m)$, where k_m usually differs slightly from k_p because the incommensurate modulation is also influence by the presence of the higher-order spatial harmonics and because the commensurate phases are additionally stabilized by the umklapp terms.[22]

When $C < 0$, the minimum of the dispersion curve $\omega^2(\mathbf{k})$ occurs along the [001] direction. Then, the ground state of the three-dimensional model (2.1) with $C < 0$ and $D > 0$ is equivalent to the ground state of the one-dimensional model analyzed in Refs. 19 and 20 with obvious substitution $k_x = k_y = 0$, which makes the dispersion

curve $\omega^2(\mathbf{k})$, Eq. (2.2), dependent on the sum $A + 4C$, B, and D.

The ground state of the three-dimensional model (2.1) shows either commensurate or incommensurate one-dimensional modulation in the z direction. Figure 1
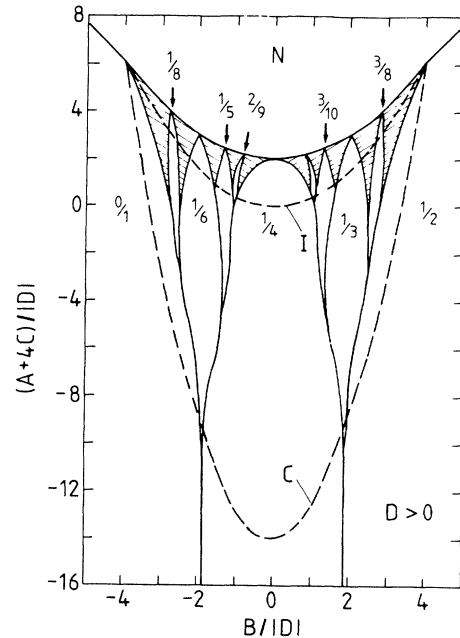
FIG. 1. Phase diagram of the three-dimensional system for $D > 0$. Each point of this diagram corresponds to a ground state of the system. By the wave vectors are indicated short-period commensurate phases. The hatched regions correspond to incommensurate phases and to long-period commensurate phases. N denotes the normal phase. Dashed lines are the paths of the incommensurate (I) and commensurate (C) cases of our model in the space of parameters, see Eqs. (2.3a)–(2.3d).

shows the phase diagram of that system at zero temperature as a function of $(A+4C)/|D|$ and $B/|D|$ for the case of $C<0$ and $D>0$. The incommensurate phases appear only if $|B/D|<4$.

We may represent the parameters of the model by more convenient quantities. This procedure will allow us to change the parameters of the potential energy so that a desired wave vector k_p of the dispersion-curve minimum can be obtained. For that we introduce the following assumptions: (i) the minimum of $\omega^2(\mathbf{k})$ should occur at the wave vector k_p along [001]; (ii) the value of the dispersion curve at its minimum, ω_0, is known; (iii) the curvatures R_x, R_y $(=R_x)$, R_z in x,y,z directions, respectively, are given and are constants, i.e.,

$$\frac{\partial \omega^2(k_p)}{\partial k_z}=0 \ , \tag{2.3a}$$

$$\omega^2(k_p)=\omega_0^2 \ , \tag{2.3b}$$

$$\frac{\partial^2 \omega^2(k_p)}{\partial k_x^2}=\frac{\partial^2 \omega^2(k_p)}{\partial k_y^2}=R_x \ , \tag{2.3c}$$

$$\frac{\partial^2 \omega^2(k_p)}{\partial k_z^2}=R_z \ . \tag{2.3d}$$

The four parameters A, B, C, and D of the harmonic part of the potential energy can now be determined through the four conditions (2.3a)–(2.3d) for given k_p, ω_0^2, R_x, and R_z. Changing within these confinements the wave vector k_p of the minimum of $\omega^2(\mathbf{k})$ one changes A, B, and D while C is fixed by R_x. The anharmonic parameter G is fixed by the value of the mean displacement $\langle u(i,j,l)\rangle \approx -\omega_0^2/(2G)$, which should be taken much less than the lattice constants. The anharmonic parameter G does not have any influence on the ground-state phase diagram.

In the following two cases of the model— an incommensurate and commensurate one—are studied. For both the parameters are $\omega_0^2=-4.0$, $C=-4.0$ (or $R_x=32\pi^2$), and $G=1000$. However, the curvatures of the dispersion curve along the modulation direction are taken to be different: they are $R_z=64\pi^2$ and $R_z=8\pi^2$ for the incommensurate and commensurate cases, respectively. A large curvature R_z causes the umklapp terms of commensurate phase, characterized by a wave vector located away from the minimum, k_p, to be unable, to stabilize the commensurate phase. A small curvature R_z assures that the contributions of umklapp terms of a simple commensurate phase always win the competition with the free energy of the pure incommensurate phase. Hence, a large or small curvature R_z increases the range of stability of incommensurate or commensurate phase, respectively. The dashed lines in Fig. 1 indicate the paths along which the system moves while k_p changes from 0 to $\frac{1}{2}$. In the incommensurate case the ground-state devil's-staircase curve, $k_m=f(k_p)$, which is just the relation between the modulation wave vector k_m at the equilibrium of the system and the parameter k_p, contains pieces of the incommensurate phases, and therefore, according to[23] should be called an incomplete-devil's-staircase curve. In
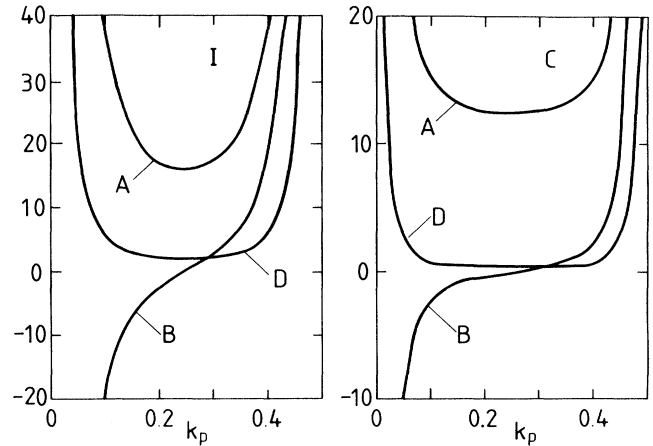
FIG. 2. The parameters A,B,D of the potential energy as a function of k_p which follows from Eqs. (2.3a)–(2.3d) for the incommensurate (I) and commensurate (C) cases.

the commensurate case, $k_m=f(k_p)$ consists of commensurate phases $\frac{0}{1},\frac{1}{6},\frac{1}{4},\frac{1}{3},\frac{1}{2}$ only and is thus called complete. Figure 2 displays the variation of the model parameters A, B, and D as a function of the wave vector k_p. Note that in the incommensurate case the couplings B and D between the first- and second-nearest neighbors remain almost an order of magnitude larger than in the commensurate model. Moreover, in our case the coupling B vanishes at $k_p=\frac{1}{4}$. Singular values of the parameters close to $k_p=0$ and 0.5 severely diminish the accuracy of the calculations in this region and thereby preclude calculations with wave-vector modulation close to the zone center or zone boundary.

The model has been studied by molecular-dynamics simulations using the technique previously described in Refs. 3 and 15. Each particle has fixed neighbors, in contrast to other molecular-dynamics simulations of incommensurate phases,[24] where diffusion of particles was allowed. Our simulated crystallite consisted of $N=40\times40\times60=96\,000$ unit cells. The Newtonian equations of motion were solved by a simple difference scheme, using the microcanonical ensemble with total energy conserved. In order to remove the surface effects periodic boundary conditions were used, although these conditions and the finite size of the crystallite[25] cause two effects: (i) The finite crystallite can admit only wave vectors $k_m=n/N_z$, which correspond to an integer number n of the modulation periods inserted into the system, where N_z is the number of unit cells in the modulation direction; thus the allowed wave vectors are separated by $\Delta k_m=1/N_z$. (ii) Periodic boundary conditions prevent nucleation of stripples at the surface of the crystal;[18] thus all stripples have to be nucleated in the bulk. Surfaces, clusters of defects, and grain boundaries of real crystals which pin the modulation might behave similarly. On the other hand, surfaces which do not pin the modulation may act as an easy place to nucleate a discommensuration and consequently they may lead to a continuous

change of the modulation wave vector.

We have set the units of length to the lattice constant $c = 1$, the particle mass $M_0 = 1$, and the dispersion-curve frequency $\omega_0 = 1$. The period $\tau_0 = 2\pi/\omega_0$, which is of the order of magnitude of the characteristic period of the phonon oscillation, plays a role of a time unit for iteration of the Newtonian equations of motion. The iteration step was chosen to be $\Delta t = 0.04\tau_0$. Similarly, the temperature (and energy) unit is $T_0 = M_0\omega_0^2 c^2$.

To describe the modulation state of the system the elastic diffraction scattering function, as measured in the diffraction experiment

$$F(\mathbf{k}) = \rho^*(\mathbf{k})\rho(\mathbf{k}) \qquad (2.4)$$

was calculated for the wave vectors $\mathbf{k} = (0, 0, n/N_z)$, where n is an integer. Here

$$\rho(\mathbf{k}) = \frac{1}{N}\sum_{i,j,l}\exp[-2\pi(\mathbf{k}\mathbf{R}(i,j,l) + k_z\langle u(i,j,l)\rangle)] \qquad (2.5)$$

and $\mathbf{R}(i,j,l)$ and $\langle u(i,j,l)\rangle$ are the position of the lattice site and the time-average displacement of the particle (i,j,l), respectively. A typical time-average interval used was $(50-100)\tau_0$. Only $F(\mathbf{k})$ along the modulation direction has been calculated. Periodic boundary conditions allow us to calculate the intensity of $F(\mathbf{k})$ at the discrete wave vectors $k = n/60$. Except the Bragg peaks at the reciprocal-lattice vectors, only sharp satellites [one point in the calculated discrete $F(\mathbf{k})$ distribution] have been observed in the incommensurate case.

The static modulation in the system depends on the wave vector k_p, potential parameters, and temperature. At low temperatures, the crystallite is in well-defined modulated state. At sufficiently high temperatures, fluctuations destroy the modulation and the system transforms into the normal phase. The order parameter of such phase transition is proportional to the average amplitude of the modulation wave which is, in turn, related to the satellite intensity. The point at which the intensity of satellite vanishes defines the transition temperature from the modulated to the normal phase. Many such runs allowed us to establish the transition temperature, which is $T = 0.005\,50$ and $0.003\,80$ for $k_p = 0.25$, increasing as $k_p \to 0$, reaching $T = 0.006\,25$ and $0.004\,40$ at $k_p = 0.10$, for the incommensurate and commensurate cases, respectively.

III. KINETIC PROCESS

In real incommensurate crystals the wave vector of the modulation shifts under varying temperature, pressure, or external field. This behavior is a consequence of a shift of the minimum of the soft mode $\omega^2(k)$ caused by the renormalization of the parameters of the effective potential energy by thermal fluctuations of degrees of freedom that otherwise are irrelevant for the incommensurate modulation. In the computer simulation one disregards the irrelevant degrees of freedom and mimics the above-mentioned behavior by simply changing the model parameters of the potential.

Each kinetic run started from an equilibrated system. The rearrangement of the particle configuration has been

achieved by changing in time the model parameters A, B, and D of the potential energy (2.1) and (2.3), so that the wave vector k_p changes with time at a constant rate dk_p/dt. During this process the kinetic energy T, which represents temperature, the average potential energy $\langle V \rangle$ and the total energy $E = T + \langle V \rangle$, the maps of average particle configurations, diffuse scattering function (2.4), and hence the wave-vector position k_m of the satellite were calculated. We note here that in our calculations the total energy remains constant only if the parameters of the potential are kept constant. However, in order to study kinetic effects we have to change the model parameters and hence k_p and, in consequence, the total energy of the system.

A. The incommensurate case

The initial temperature of that run was about $0.26T_c$, where T_c is the transition temperature from the incommensurate to the normal phase and the initial parameters of the potential were fixed by $k_p = 0.40$. Figure 3 shows some results of the kinetic process which started from the initial state and was continued at a constant rate of change, $dk_p/dt = -1.5\times10^{-5}\tau_0^{-1}$. Effects related with different rates of change, dk_p/dt, have been discussed in a previous paper.[16] We see in Fig. 3(a) that the average total energy changes continuously but the temperature and average potential energy show several sharp discontinuities, Fig. 3(b), although the overall behavior remains similar to that of E. The satellite position k_m, Fig. 3(c) as given by the maximum of the diffraction scattering func-
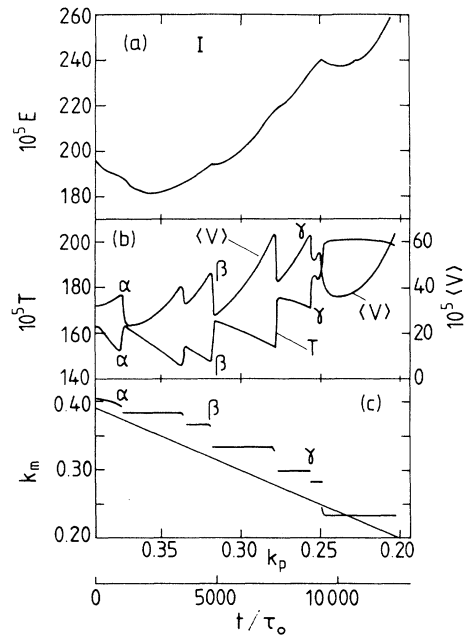
FIG. 3. (a) Total energy E, (b) temperature T and average potential energy $\langle V \rangle$, (c) diffraction satellite position k_m, as a function of the wave vector k_p and time t for the incommensurate case and for a kinetic run from $k_p = 0.4$ to 0.2 at the rate of change $dk_p/dt = -1.5\times10^{-5}\tau_0^{-1}$. The line $k_m = k_p$ is the equilibrium line of the incommensurate phase.

tion $F(\mathbf{k})$, changes stepwise at the same instants as those of T and $\langle V \rangle$. Within the resolution $\Delta k = \frac{1}{60} = 0.0167$ no broadening of the satellites was observed. Inspecting details of the maps of particle configurations we could establish that along each plateau of Fig. 3(c) the crystallite was free of stripples. Each discontinuity in the satellite position k_m was related with nucleation and growth of a stripple. The steps in Fig. 3(c) can give an erroneous impression that the model possesses commensurate phases only. In fact, these plateaus arise because of the discretization of wave vectors introduced by the finite size of the system and periodic boundary conditions.

The discontinuities observed in T and $\langle V \rangle$, Fig. 3(b) are of the following origin. Changing k_p and the parameters of the potential energy but not the number of the modulation periods in the crystallite, one increases the average potential energy $\langle V \rangle$, because the current modulation k_m is no longer at the minimum of the potential. When thermal fluctuations nucleate a stripple, this metastable state is changed by one period of the modulation and it relaxes to a state characterized by a different allowed wave vector. Simultaneously, the excess potential energy is converted into kinetic energy which causes a sudden increase in temperature. A similar effect has been observed in the reverse process when the wave vector k_p increased from 0.25 to 0.40.

The plateaus of the satellite positions, Fig. 3(c), significantly deviate from the equilibrium line. This line describes the modulation wave vector in an infinite incommensurate system except in the vicinity of the commensurate wave vector $k_p = 0$ and $\frac{1}{4}$. The deviation leads to a so-called global hysteresis and is caused by the critical energy needed to nucleate a stripple. We recall that in a three-dimensional system the stripple must exceed a critical size and critical energy before it can grow.

Below we discuss the events which occur at the discontinuities α, β, γ in Fig. 3(c). The maps of these events, namely, some X-Z and X-Y planes of the crystallite, are shown in Figs. 4, 5, and 6, respectively. The maps have been made from square and triangle symbols, sizes of which are proportional to the positive or negative average displacements $\langle u(i,j,l) \rangle$, respectively. Because of a large number of particles and consequently small available space for representing one symbol, one can see on the maps only the magnitude of the particle-displacement amplitudes. Due to that, however, one can recognize dark and white regions, which correspond to large and small particle displacements or, in other words, to domains and domain walls (discommensuration planes), respectively. The X-Z planes cross the center of the crystallite and show the particle configurations along the modulation direction z. The X-Y maps visualize the stripple evolution in planes perpendicular to the modulation direction and lay at the level indicated by the side marks on the X-Z maps. Notice that the time period of $(10-12)\tau_0$, during which the stripple evolves, is related to the velocity of the deperiodization line and is very short in comparison to the total time of duration $12\,500\tau_0$, of the whole kinetic process.

Consider the defect appearing at the discontinuity α, Fig. 3(c). On the first map, Fig. 4(a), the incommensurate
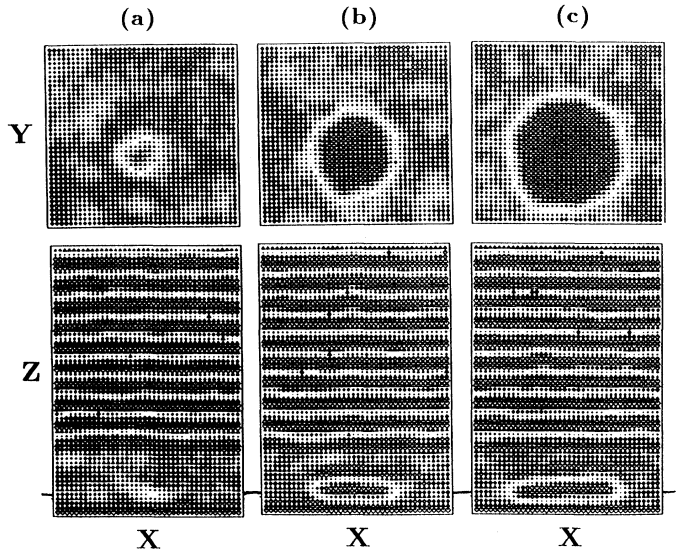
FIG. 4. Maps of particle configurations of the incommensurate case around $k_p = 0.3731$ at the discontinuity α in Figs. 3(b) and 3(c), which demonstrate the nucleation and growth of the stripple within a region of a commensurate phase $k = \frac{1}{2}$. The time increment between maps is $\Delta t = 4\tau_0$.

and commensurate $k = \frac{1}{2}$ phases coexist and the moment of stripple nucleation is seen. It grows in lateral directions as seen in the maps, Figs. 4(b) and 4(c). Its deperiodization line, a closed circle, is visible in the X-Y planes. The structure of this stripple is very simple. Inside, it possesses a domain opposite to the one which fills the space outside the stripple. Its reference commensurate phase, which in this case is the phase $k = \frac{1}{2}$, has two domains only. Notice that the stripple, Fig. 4, has appeared close to the incommensurate region at the top of the X-Z plane (we recall that the bottom of the crystallite is close to its top because of periodic boundary conditions) and not at the middle part of the commensurate domain, preserving in this way the correct separation between the discommensuration planes. Another stripple, already noticed in Fig. 4(c), has grown a moment later and it has filled the remaining region of the commensurate domain $k = \frac{1}{2}$. Thus, the discontinuity α is attributed to two stripples. The radial velocity of the deperiodization line, estimated from the X-Y maps of Fig. 4, is $dr/dt = 1.8a/\tau_0$. This value can be compared with the phason velocity $v_{\mathrm{ph}} = 2.8a/\tau_0$ inferred from the theoretical slope of the phason dispersion branch of our model [see Eq. (8.8) of Ref. 3]. In an order-disorder system the velocity of the deperiodization line, described then by a local relaxation processes, can be orders of magnitude slower. A discussion of physical consequences of these effects can be found in.[25]

The discontinuity β in Fig. 3(c) is caused by two antistripples, which pass the crystallite one after another. They transform the incommensurate phase $k_m = 0.367$
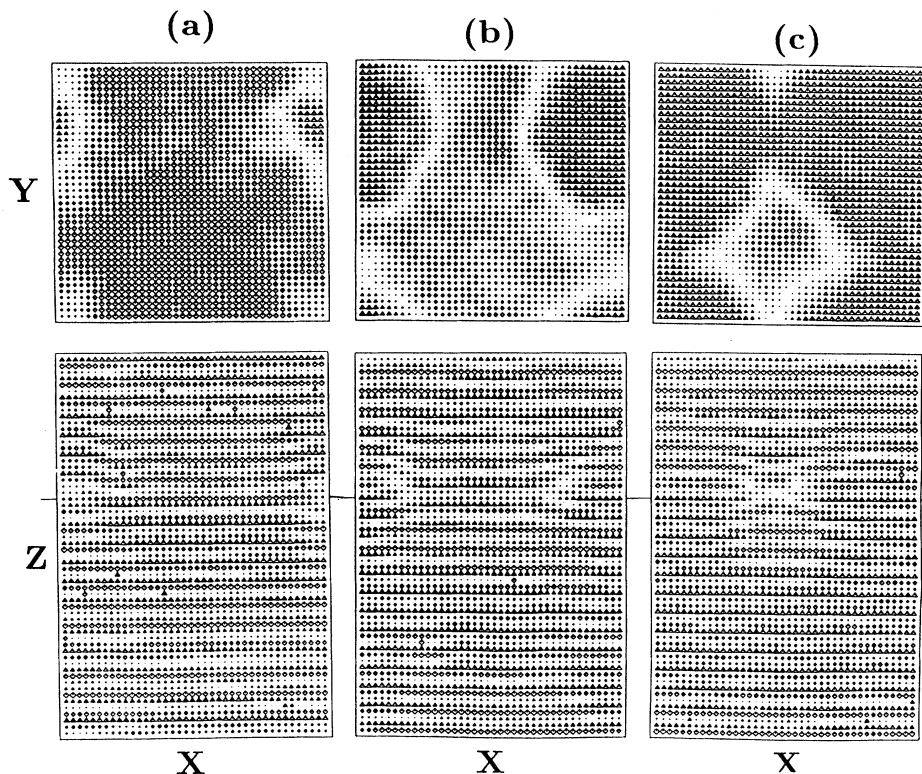
FIG. 5. Maps of particle configurations of the incommensurate case around $k_p = 0.3174$ at the discontinuity β in Figs. 3(b) and 3(c), which demonstrate the nucleation of a partial antistripple $I \rightarrow \frac{1}{3}$. The time increment is $\Delta t = 6\tau_0$. The scheme of domain patterns is given in Fig. 7.

into a domain of commensurate phase $k = \frac{1}{3}$. The maps of evolution of the second antistripple at the discontinuity β are shown in Fig. 5. The closed discommensuration line of the antistripple is seen in the X-Y maps. The antistripple has nucleated close to the edges of the X-Z

map, Fig. 7(a), and then it propagates. The radial velocity of the deperiodization line, as inferred from X-Y maps of Fig. 5, is $dr/dt = 1.3a/\tau_0$.

The phase $k = \frac{1}{3}$ may exist in six domains.[3] If we describe the periodic modulation as
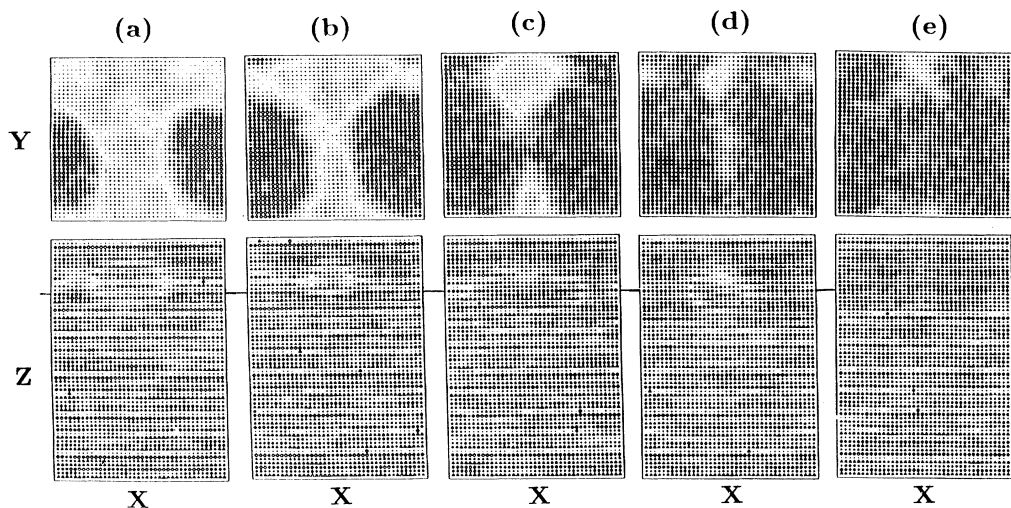
FIG. 6. Maps of particle configuration of the incommensurate case around $k_p = 0.2562$ at the discontinuity γ in Figs. 3(b) and 3(c), which demonstrate the existence of defects in the lattice during its reconstruction from phase $k = \frac{3}{10}$ to $k = \frac{1}{4}$. The time increment is $\Delta t = 2\tau_0$. The scheme of domain patterns is given in Fig. 8.
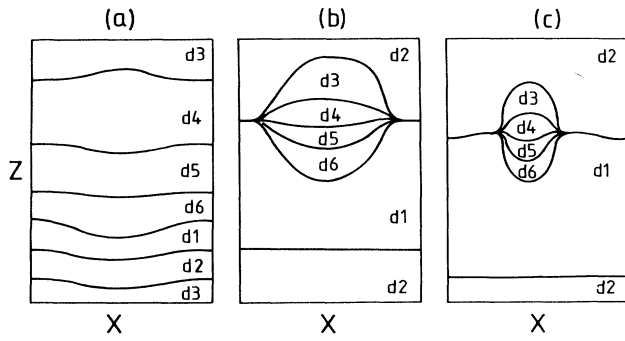
FIG. 7. Scheme of the domain patterns at the transition from the incommensurate to the commensurate phase $k = \frac{1}{3}$ demonstrating an evolution of partial antistripple. The patterns represent the particle configurations on the X-Z maps of Fig. 5. The particle displacements $+--$, $++-$, $-+-$, $-++$, $--+$, $+-+$ are the characteristic patterns of $d1$, $d2$, $d3$, $d4$, $d5$, and $d6$ domains of commensurate phase $k = \frac{1}{3}$, respectively.

$$\langle u(i,j,l) \rangle = A \cos[2\pi \mathbf{k} \cdot \mathbf{R}(i,j,l) - \epsilon] , \tag{3.1}$$

where A is the amplitude of the modulation, then the phase shifts of the six domains of the commensurate phase $k = \frac{1}{3}$ are $\epsilon = 0$, $\pi/3$, $2\pi/3$, π, $4\pi/3$, and $5\pi/3$. We denote these domains by $d1$, $d2$, $d3$, $d4$, $d5$, and $d6$, respectively. The domain walls or discommensuration planes between domains with the smallest difference in phase $\Delta\epsilon = \pi/3$ are expected to have the lowest energy. Figure 7 shows hand-drawn schematic pictures of the sequence of domains made in a simplified way, namely, by comparing the sequence of signs of particle displacements of the X-Z map of Fig. 5 with the standard sequence of signs of displacements of domains of the phase $k = \frac{1}{3}$. A full antistripple imbedded into domain $d1$ should consist of six discommensuration planes which separates the remaining five domains $d2$, $d3$, $d4$, $d5$, $d6$, and all the discommensuration planes should meet at the deperiodization line. In our case, however, the system has produced a *partial antistripple,* Figs. 5(b) and 5(c) and Figs. 7(b) and 7(c), which consists of only four domains $d3$, $d4$,

$d5$, $d6$, and reduces five discommensuration planes to one $d2/d1$. Indeed, for wave vectors $k_p > \frac{1}{3}$ the antistripple structure requires an ordered sequence of domains $d1$, $d2, \ldots, d6$. Discommensuration plane with the reverse order of domains, like $d2/d1$, then has higher energy and in normal conditions should not appear. However, at the moment of β discontinuity, our model is already in state $k_p < \frac{1}{3}$, where stripples with reverse sequence of domains $d6$, $d5, \ldots, d2$, $d1$ are energetically favored. In these circumstances the system prefers to nucleate a partial antistripple, which produces finally one discommensuration plane $d2/d1$ and which already satisfies the order of domain sequence required at $k_p < \frac{1}{3}$.

When the value of $k_p = 0.276$ is reached, two stripples, based on the commensurate phase $k = \frac{1}{3}$, are generated. As a result, a perfect commensurate phase $k = \frac{3}{10}$ is produced. Later on, at the γ discontinuity when $k_p = 0.256$, a topological defect, shown on the maps of Figs. 6 and 8, passed through the crystallite. In X-Y maps, Fig. 6, the evolutions of the deperiodization lines are clearly seen. The analysis of the domain pattern is, however, not so straightforward. At Figs. 8(a) and 8(b) and Figs. 8(c)–8(e) the hand-drawn scheme of the domain sequences are described by comparing the signs of the particle displacments with the signs of the domain patterns of the commensurate phases $k = \frac{1}{3}$ and $k = \frac{1}{4}$, respectively. The commensurate phase $k = \frac{1}{4}$ may exist in four domains described by the phase shift $\epsilon = \pi/4$, $3\pi/4$, $5\pi/4$, and $7\pi/4$. We denote the corresponding domains by $D1$, $D2$, $D3$, and $D4$, respectively. In Fig. 8(a) the sequence of domains corresponds to phase $k = \frac{3}{10}$. A stripple based on the commensurate phase $k = \frac{1}{3}$ starts to nucleate at the edges of the crystallite. However, this stripple does not encompass yet all domains. A moment later a little modification of particle displacements within the stripple allows one to recognize the domains $D3$ and $D4$ of the commensurate phase $k = \frac{1}{4}$, Fig. 8(c). The domain $D4$ is confined between two $D3$ domains. Normally, the domains must form a directed sequence in order to achieve the minimum in potential energy. That means the discommensurations $D3/D4$ and $D4/D3$ are of different energies. In our case, however, the wave vector
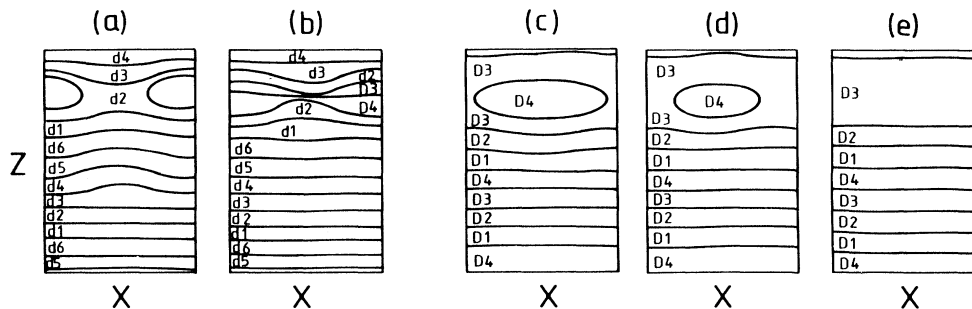
FIG. 8. Scheme of the domain patterns at the transition from phase $k = \frac{1}{3}$ toward the commensurate phase $k = \frac{1}{4}$. The patterns reflect the particle configurations on the X-Z maps of Fig. 6 and are described in terms of domains $d1$–$d6$ and $D1$–$D4$ of commensurate phases $\frac{1}{3}$ and $\frac{1}{4}$, respectively. The particle displacements $++--$, $-++-$, $--++$, $+---+$ are the characteristic patterns for $D1$, $D2$, $D3$, and $D4$, domains of phase $k = \frac{1}{4}$, respectively.

k_p is close to $\frac{1}{4}$, and at $k_p = \frac{1}{4}$ the discommensuration planes becomes energetically equivalent.

Later on the island of the domain $D4$ disappears due to the typical antistripple mechanism and finally a region of single commensurate domain of the phase $k = \frac{1}{4}$ is formed. The lifetime of the region of a single domain is rather short since the remaining discommensurations planes shift into the z direction in order to achieve an equidistance separation.

The discontinuity γ is an example of topological defects within the intermediate region between two simple commensurate phases, where stripple structure based on one reference commensurate phase, say $k = \frac{1}{3}$, becomes imperfect and description of the same region of the crystal, by domains of another reference commensurate phase, say $k = \frac{1}{4}$, becomes more appropriate. It is obvious that such a change in description must occur somewhere when the wave vector changes from one commensurate phase to another.

B. The commensurate case

In the commensurate case the model is strongly anisotropic. The interaction between particles in the z direction is an order of magnitude smaller than in x and y. The kinetic process, which started from an initial single domain of commensurate phase $k = \frac{1}{3}$ being at temperature $0.66T_c$, was continued at a constant rate of change, $dk_p/dt = -5.0 \times 10^{-5} \tau_0^{-1}$. The average total energy remained almost constant, Fig. 9(a), and the temperature and average potential energy, Fig. 9(b) exhibit changes around $k_p = 0.25$ correlated with the coexistence of two satellites at $k_m = \frac{1}{3}$ and $k_m = \frac{1}{4}$, Fig. 9(c). Here, the commensurate-commensurate phase transition $\frac{1}{3} \rightarrow \frac{1}{4}$ takes place. Note that in spite of more than three times faster rate then used in the run of the incommensurate case, this phase transition requires a considerably longer time of $210\tau_0$ to complete. In Fig. 12 we present maps of particle configurations taken during this process. We have tried as before, to assign to the signs of particle displacements of the X-Z maps of Fig. 10, the signs of the domain pattern of the commensurate phases $k = \frac{1}{3}$ and $k = \frac{1}{4}$. And indeed one sees that the first X-Z map belongs 90% to a single domain of phase $k = \frac{1}{3}$. This can be shown in spite of rather large fluctuations which diminish the averaged values of particle displacements in random parts of the crystallite. In the course of time, however, many new domains arise but they *do not* form a sequence expected for a stripple.

On the X-Y maps of Fig. 10 which represent layers of crystallite perpendicular to the modulation direction, one sees closed line which separate regions with opposite displacements of particles. We call such a line a kink line. The region confined by a kink line can be called a *planar nucleus*. The kink line has properties similar to the deperiodization line. The planar nucleus grows, in principle, within one X-Y layer of the crystal, where the interactions are strong. The nucleation and growth of planar nuclei in neighboring layers may be correlated.

In this commensurate case the stripple mechanism has
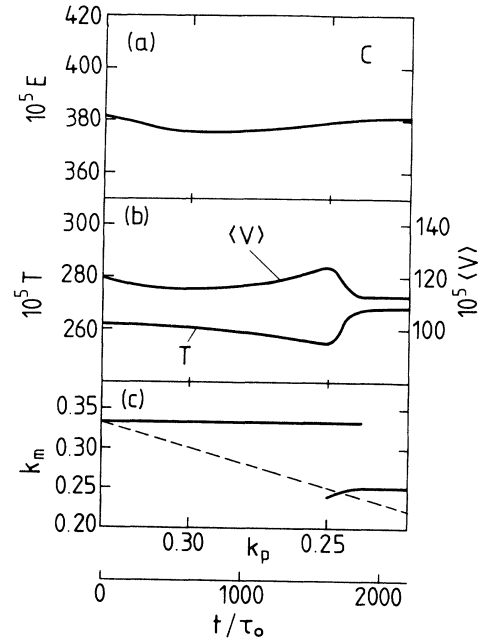
FIG. 9. (a) Total energy E, (b) temperature T and average potential energy $\langle V \rangle$, (c) position of the diffraction satellite k_m as a function of the wave vector k_p and time t for the commensurate case and for a kinetic run from $k_p = 0.333$ to 0.220 at a rate of change $dk_p/dt = -5.0 \times 10^{-5}\tau_0^{-1}$. The line $k_m = k_p$ is a guide to the eye.

not been observed. Therefore, we indicate on the schematic pictures of Fig. 11 only planar nuclei which have been grown on the maps of Fig. 10 and in which the average particle displacements are opposite to displacements required by the initial single domain of phase
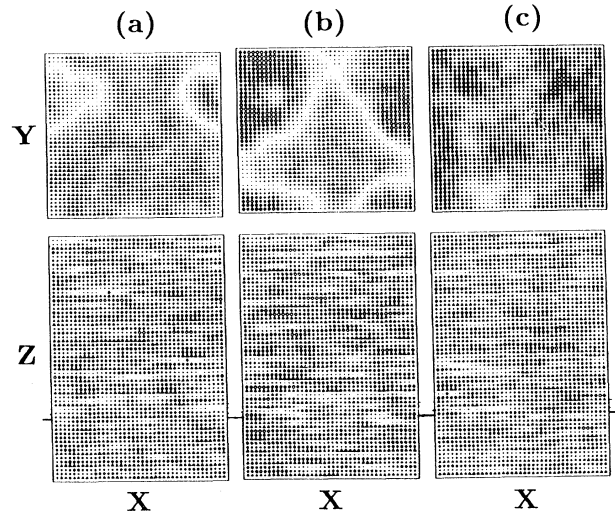
FIG. 10. Maps of particle configurations of the commensurate case at the discontinuity in Figs. 9(b) and 9(c), which demonstrate the lattice reconstruction at the transition from commensurate phase $k = \frac{1}{3}$ to commensurate phase $k = \frac{1}{4}$. The wave vector k_p from (a) to (c) changes from 0.2496 to 0.2481 and the time increment between maps is $\Delta t = 10\tau_0$.
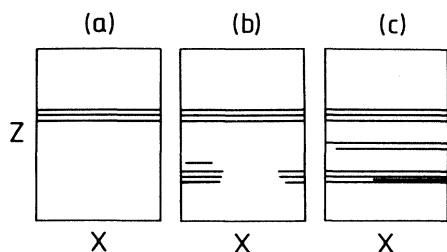
FIG. 11. Scheme of the planar nuclei made on the basis of the X-Z maps of Fig. 10, with the initial domain of phase $k = \frac{1}{3}$ taken as a reference configuration.

$k = \frac{1}{3}$. Obviously, the density of planar nuclei increases with time. These objects form local thin domains which correspond to the commensurate phase $k = \frac{1}{4}$. At this intermediate stage the diffraction pattern of the whole system consists of two satellites placed at $k_m = 0.333$ and $k_m = 0.25$, and the growing one at $k = 0.25$ was broadened and reached a maximum width of about $\Delta k_m = 0.04$. Later on, some of the domains have increased their volumes at the expense of the remaining domains and the diffraction spectrum coalesced into a single satellite at $k_m = 0.25$

IV. FINAL REMARKS

The results of simulations confirm the existence of the stripple mechanism in the incommensurate case of a three-dimensional model crystal, where the coupling parameters along the modulation direction are of the same order of magnitude as the couplings within the plane perpendicular to it. Generally, the stripples have a structure determined by the domains of the reference commensurate phase, similar to the stripples observed experimentally with electron-microscope techniques. In the commensurate case, having a weak coupling along the modulation direction, any attempt to form a stripple is immediately thwarted by thermal fluctuations. However, the strong couplings within the plane perpendicular to the modulation direction lead to nucleation and growth of planar nuclei.

The kinetic devil's-staircase curve of the incommensurate case obtained during a single kinetic run, Fig. 3(c), showed a hysteresis and proved to have some discontinui-

ties. If in a macroscopic system the stripples will appear at random, then the discontinuities would occur at random as well and consequently the average wave-vector dependence may prove to behave continuously,[16] in agreement with some experimental observations. However, a global hysteresis which depends on the critical nucleation energy of the stripple and not on the size of the system should be observed.

Because of obvious reasons of limited computer time we have applied periodic boundary conditions to minimize the effect of crystal surfaces. This conditions have discretize the wave vectors; therefore plateaus of satellite positions in Fig. 3(c) occur at a well-defined wave vectors only. The effect of discretization will diminish with increasing crystallite. Another effect of the periodic boundary conditions seems to be more important. This conditions prevent the nucleation of stripples at the surface of the crystallite. A strong pinning of the modulation-wave amplitude at the free surface of the crystal will cause a similar effect of forcing nucleation in the bulk, independent of the system size. The influence of the boundary conditions on stripple nucleation has been published in a separate paper.[18]

Indications that not everything is understood in the problem of the wave-vector changes in incommensurate systems come from the dielectric and birefringencey measurements made on the thiourea doped with 3% of urea[26] and quartz,[27] respectively, at an extremely slow heating rate. The data show that the modulation wave vector changes not in a continuous way, as the majority of experiments would suggest, but in a stepwise way and that the steps have nothing to do with the commensurability of the lattice. This behavior is usually attributed to defects which might imitate in an extremely crude way the effect of periodic or fixed boundary conditions.

ACKNOWLEDGMENTS

*Permanent address: Institute of Nuclear Physics, ul.Radzikowskiego 152, PL-31-342 Kraków, Poland.

[1] V. Janovec, Phys. Lett. **99**, 384 (1983).

[2] K. Kawasaki, J. Phys. C **16**, 6911 (1983).

[3] K. Parlinski, Comp. Phys. Rep. **8**, 153 (1988).

[4] G. André, D. Durand, F. Dénoyer, R. Currat, and F. Moussa, Phys. Rev. B **35**, 2909 (1987).

[5] H. G. Unruh, J. Phys. C **16**, 3254 (1983).

[6] J. P. Jamet and P. Lederer, J. Phys. (Paris) **44**, L257 (1983).

[7] K. Hamano, H. Sakata, and K. Ema, J. Phys. Soc. Jpn. **56**, 3789 (1987).

[8] H. Sakata, K. Hamano, and K. Ema, J. Phys. Soc. Jpn. **57**, 4242 (1988).

[9] G. Eckold, Nucl. Instrum. Methods Phys. Res. **A289**, 221 (1990).

[10] K. K. Fung, S. McKernem, J. W. Steeds, and J. A. Wilson, J. Phys. C **14**, 5417 (1981).

[11] C. N. Chen, J. M. Gibson, and R. M. Fleming, Phys. Rev. B **26**, 184 (1982).

[12] H. Bestgen, Solid State Commun. **58**, 197 (1986).

[13]S. Barre, H. Mutka, and C. Roucau, Phys. Rev. B **38**, 9113 (1988).

[14]M. Ribet, Ferroelectrics **66**, 259 (1986).

[15]K. Parlinski, Phys. Rev. B **35**, 8680 (1987).

[16]K. Parlinski, Phys. Rev. B **39**, 12 154 (1989).

[17]A. Joets and R. Ribotta, J. Phys. (Paris) **47**, 595 (1986).

[18]K. Parlinski and F. Dénoyer, Phys. Rev. B **41**, 11 428 (1990).

[19]T. Janssen and J. A. Tjon, Phys. Rev. B **25**, 2245 (1981).

[20]J. J. M. Slot and T. Janssen, Physica D **32**, 27 (1988).

[21]W. Selke, Phys. Rep. **170**, 213 (1988).

[22]K. Parlinski and F. Dénoyer, J. Phys. C **18**, 293 (1985).

[23]S. Aubry, in *Solitons and Condensed Matter Physics*, edited by A. R. Bishop and T.-Schneider (Springer, New York, 1978), p. 264.

[24]C. Z. Wang, E. Tosatti, and A. Fasolino, Phys. Rev. Lett. **60**, 2661 (1988).

[25]K. Parlinski, Ferroelectrics **104**, 73 (1990).

[26]A. Onodera, F. Dénoyer, J. Godard, and M. Lambert, J. Phys. (Paris) **49**, 2065 (1988).

[27]F. Mogeon, G. Dolino, and M. Vallade, Phys. Rev. Lett. **62**, 179 (1989).